



This is a repository copy of *An Exceptional Summer during the South Pole Race of 1911-1912*.

White Rose Research Online URL for this paper:
<https://eprints.whiterose.ac.uk/116051/>

Version: Supplemental Material

Article:

Fogt, R. L., Jones, M. E., Solomon, S. et al. (2 more authors) (2017) An Exceptional Summer during the South Pole Race of 1911-1912. *Bulletin of the American Meteorological Society*, 98 (10). pp. 2189-2200. ISSN 0003-0007

<https://doi.org/10.1175/BAMS-D-17-0013.1>

Reuse

Items deposited in White Rose Research Online are protected by copyright, with all rights reserved unless indicated otherwise. They may be downloaded and/or printed for private study, or other acts as permitted by national copyright laws. The publisher or other rights holders may allow further reproduction and re-use of the full text version. This is indicated by the licence information on the White Rose Research Online record for the item.

Takedown

If you consider content in White Rose Research Online to be in breach of UK law, please notify us by emailing eprints@whiterose.ac.uk including the URL of the record and the reason for the withdrawal request.



eprints@whiterose.ac.uk
<https://eprints.whiterose.ac.uk/>

1 Figure S1 demonstrates that along the sledging journeys, despite only a few observations
2 per day, the same general story emerges whether daily means or maximum or minimum
3 temperatures are used. Since the sign of temperature anomalies switched during the
4 journey, with temperatures above average for much of December, but notably below
5 average for January as well as late February / early March for Scott, we use daily
6 averages rather than a combination of daily maximum and daily minimum temperatures.

7
8 Figure S2 shows the mean climatological cycle of 2 m temperature over the Ross Ice
9 Shelf region from ERA-Int. The values are in close agreement with Costanza et al.
10 (2016), including the colder air near Roosevelt Island that extends westward toward the
11 Transantarctic mountains in all months, and the warmer air descending down the major
12 glacial valleys in the Transantarctic mountains, most marked in October- November and
13 February – March.

14
15 The model elevations for the $0.75^{\circ} \times 0.75^{\circ}$ resolution ERA-Int data under-represent the
16 complex and steep terrain in the vicinity of the Transantarctic mountains (compare Fig. 1
17 from main paper with Fig. S3). Using a standard environmental lapse rate of 6.5°C per
18 km, the 2m temperatures in ERA-Int were adjusted to the correct elevations along the
19 sledging journeys for both Amundsen and Scott. Despite the differences in regions of
20 steep terrain and the glacial valleys, the elevation-corrected climatological temperature
21 data agrees well with the conditions experienced by both polar parties (Fig. S4); most
22 sledging observations fall within the 30-year temperature variability and absolute range
23 provided from the elevation-corrected ERA-Int data.

24
25 The pressure reconstruction at Amundsen-Scott (Fig. S5) from Fogt et. al (2016a,b), like
26 at McMurdo, shows that the summer of 1911/1912 is one of the highest points for the
27 entire reconstruction and observation period. The reconstruction value is slightly above
28 692 hPa, and although the reconstructed values have pressure this high multiple times,
29 the observations only have a similar value two times during 1957-2013. The Amundsen-
30 Scott pressure reconstruction is similarly reliable, with a calibration correlation value of
31 $r=0.859$. When considering this with the McMurdo pressure reconstruction, and the same
32 large positive spike during this season, we are more confident in the exceptional nature of
33 this season, especially along the routes of both Amundsen and Scott. All available early
34 gridded pressure datasets indicate this was a season of very high pressure across the
35 entire Antarctic continent, reflecting a negative phase of the Southern Annular Mode
36 (Fig. S6).

37
38 One of the common assumptions made in this paper is that pressure values from
39 McMurdo, Cape Evans, and Framheim are comparable to conditions across the Ross Ice
40 Shelf (Barrier). Figure S7 shows the relationships between different regions of Antarctica
41 compared to McMurdo, with Fig. S7a illustrating correlations of $r=0.99$ across much of
42 the Ross Ice Shelf. Fig. S7b shows the root mean squared error (RMSE), with the lowest
43 values in this same region (primarily along Scott's route on the Barrier) when comparing
44 both plots. In the original paper, Fig. 2a is a comparison of pressure on the barrier
45 between the sledging parties and the two bases, with the McMurdo 1981-2010
46 climatological mean and ± 2 standard deviations. The barrier is defined as any

47 observations taken at elevations below 100 m, and the sledging parties' observations
48 match up very well with the data from Cape Evans and Framheim. Fig S7 demonstrates
49 that these are fair comparisons, since the pressure correlation between the Ross Ice Shelf
50 and the Ross Island area is near unity. Although a bit weaker, the correlations are still
51 high and the RMSE is still low from the Transantarctic Mountains southward to the South
52 Pole with those at the Ross Island area, allowing for comparison with notable skill of the
53 pressures at Cape Evans / Framheim all the way to the South Pole in summer.

54
55 Figure S8 demonstrates that while there is a significant relationship using seasonal mean
56 data between the SAM index and temperature across Antarctica (Marshall 2007), the
57 relationship using monthly data is primarily insignificant across the Ross Ice Shelf,
58 except in November and February. Therefore the higher pressures observed by the field
59 parties and at Cape Evans and Framheim may not necessarily have a corresponding
60 strong temperature anomaly associated with them, especially when on the Ross Ice Shelf.
61 During much of January when pressures were lower, it is not surprising also to see
62 weaker temperature anomalies by both parties, as well as the lack of simultaneous strong
63 temperature anomalies as noted in early December 1911.

64
65 The warm temperatures Amundsen experienced in early December are compared to the
66 10-minute quality controlled temperatures from the closest automatic weather station,
67 Henry AWS (-89.0°S, -0.39W) using daily maximum temperatures in Fig. S9. The
68 values on December 5-6 recorded by Amundsen stand out as very warm conditions,
69 which have only been recorded at Henry AWS later in the month.

70
71 Figure S10 demonstrates the sensitivity to the length and duration of the time windows
72 chosen to contrast the warm temperatures in early February 1912 to the cold temperatures
73 in late February / early March 1912, and is based on the original data (similar structure as
74 in the main manuscript is observed when using anomaly data). We used differing lengths
75 for the number of days included for both the early and late time periods (from as little as
76 4 consecutive days to as long as 15 consecutive days, termed the 'windows') over which
77 temperatures were averaged. We then took the difference of all these averages, and
78 generated a histogram. The time windows for the early period encompass all or portions
79 of February 9-15 for the earlier period, and February 27 – March 5 for the later period.
80 For window lengths over the original 7 days length, the windows were generated such
81 that they extended evenly outside the original 7-day periods, and as such for even length
82 day windows above 6, two subsets were created: one that had an extra day at the
83 beginning of each time period, and one that had an extra day at the end of each time
84 period. The histograms there have larger counts for all the differences for even numbered
85 windows >6, and for smaller windows <7. The red vertical line shows the average
86 temperature difference experienced by Scott during the same periods. Regardless of how
87 the time windows are chosen, it is seen that the temperature change experienced by Scott
88 during this time was in the top <3% of the data distribution based on ERA-Int data,
89 highlighting its uniqueness.

90
91
92

93
94
95
96
97
98
99
100
101
102
103
104
105
106
107
108
109
110
111
112
113
114
115
116
117
118
119

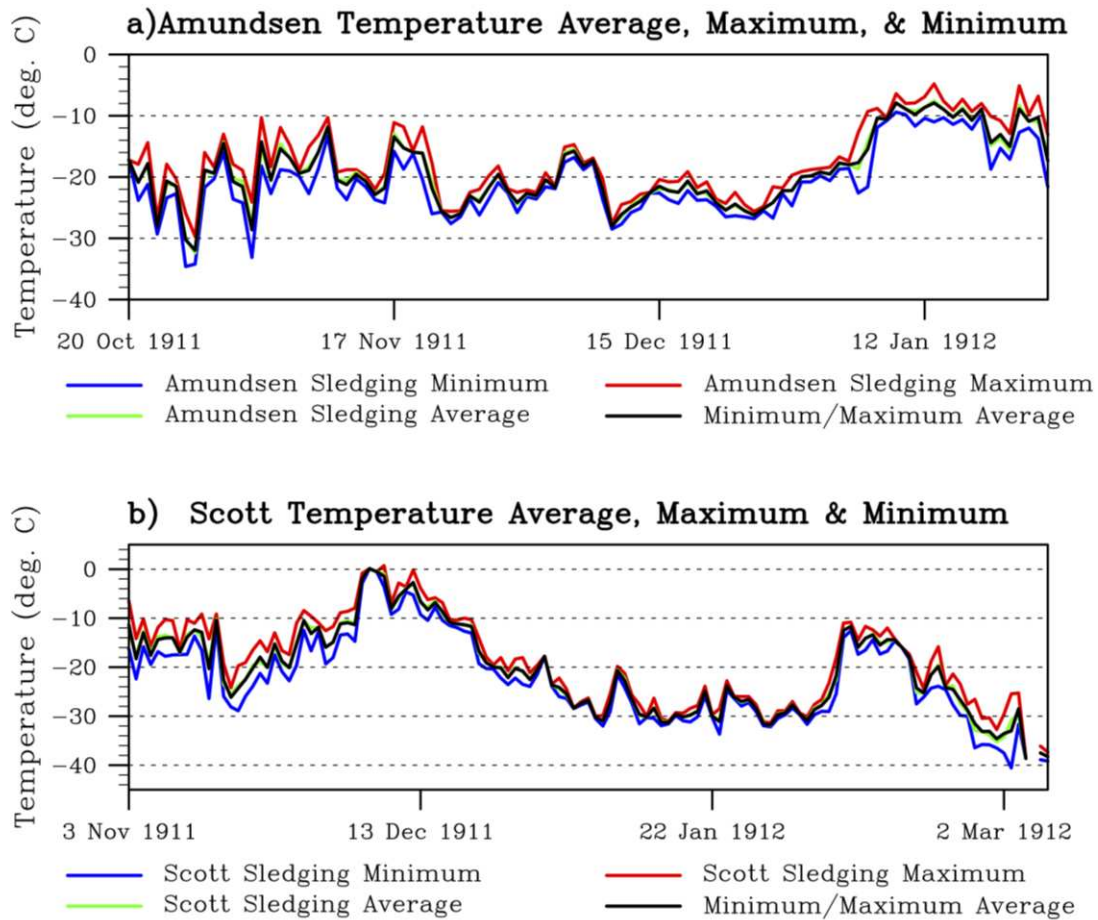
References

Costanza, C. A., M. A. Lazzara, L. M. Keller, and J. J. Cassano, 2016: The surface climatology of the Ross Ice Shelf Antarctica. *Int. J. Climatol.*, doi:10.1002/joc.4681.

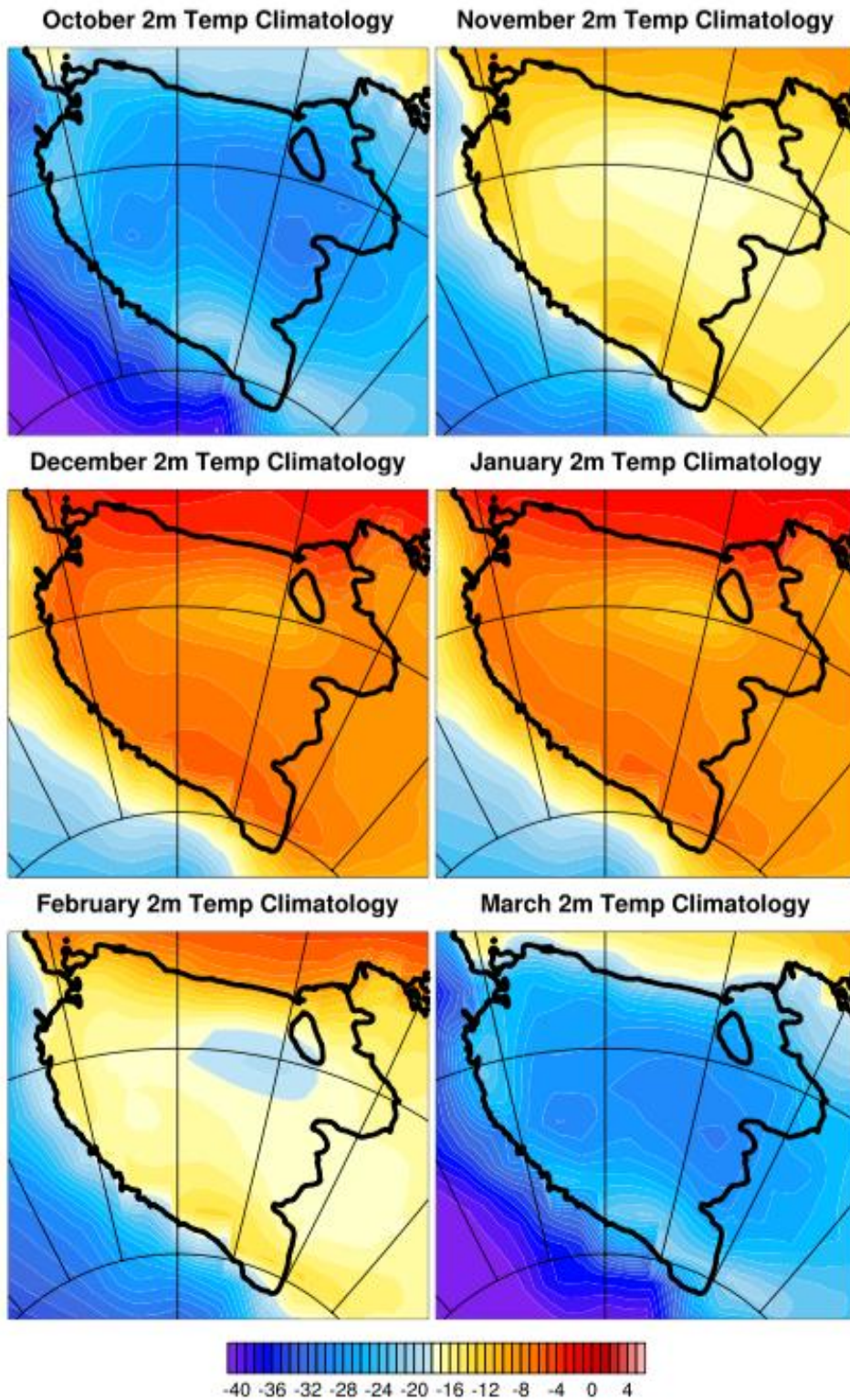
Fogt, R. L., C. A. Goergens, M. E. Jones, G. A. Witte, M. Y. Lee, J. M. Jones, 2016a: Antarctic station-based seasonal pressure reconstructions since 1905: 1. Reconstruction evaluation. *J. Geophys. Res.*, **121**, 6, 2814.

Fogt, R. L., J. M. Jones, C. A. Goergens, M. E. Jones, G. A. Witte, M. Y. Lee, 2016b: Antarctic station-based seasonal pressure reconstructions since 1905: 2. Variability and trends during the twentieth century. *J. Geophys. Res.*, **121**, 6, 2836.

Marshall, G. J., 2007: Half-century seasonal relationships between the southern annular mode and Antarctic temperatures. *Int. J. Climatol.*, **27**, 373–383.

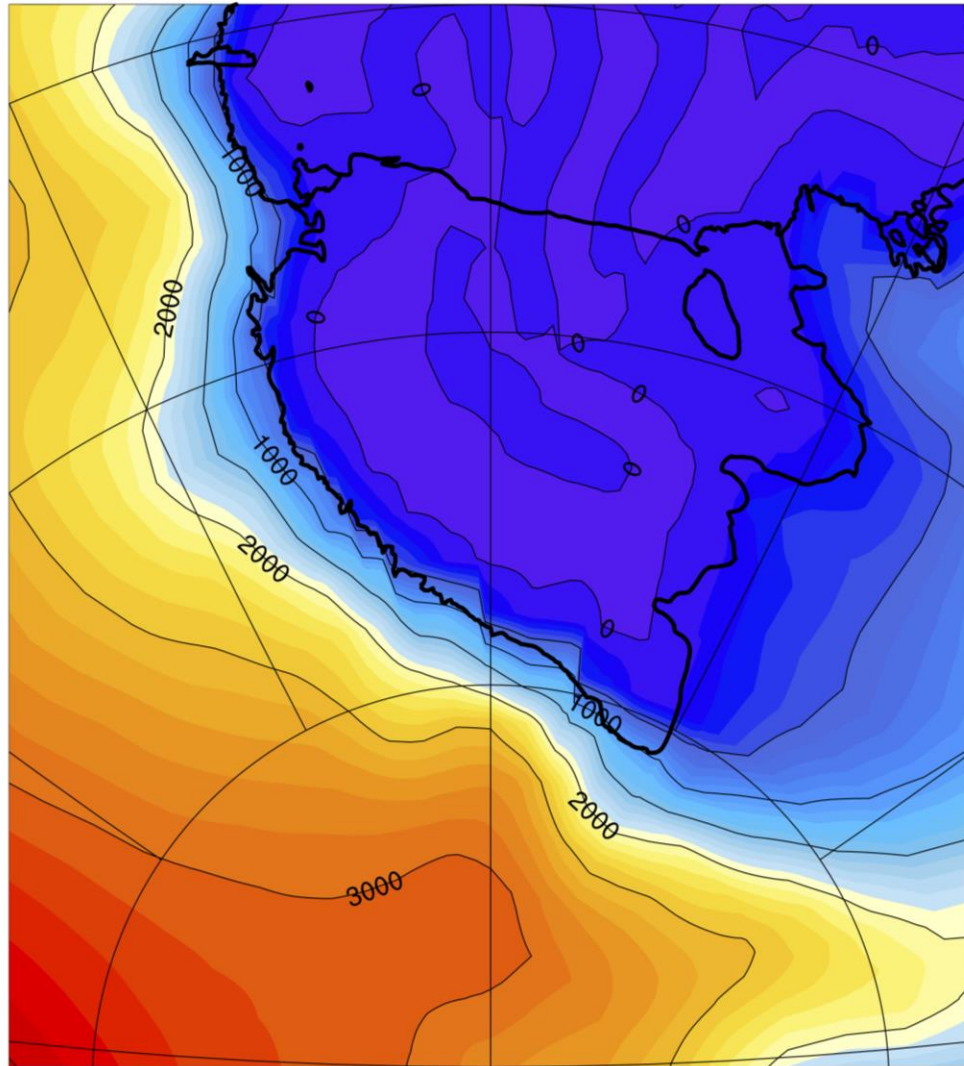


120 **Figure S1.** Time series of daily mean, maximum, and minimum temperatures along the
 121 sledging journey for a) Amundsen and b) Scott. Also shown is the average of the daily
 122 maximum and minimum (black line), which agrees closely with the average of all
 123 observations (green), further providing support that using the daily mean of the limited
 124 number of observations does not bias the interpretation of the temperature variability
 125 during the sledging journeys.
 126



127 **Figure S2.** ERA-Int 2m temperature (in °C) climatology by month, October – March,
 128 averaged during 1981-2010.

ERA-Interim 0.75x0.75 Elevation (m)

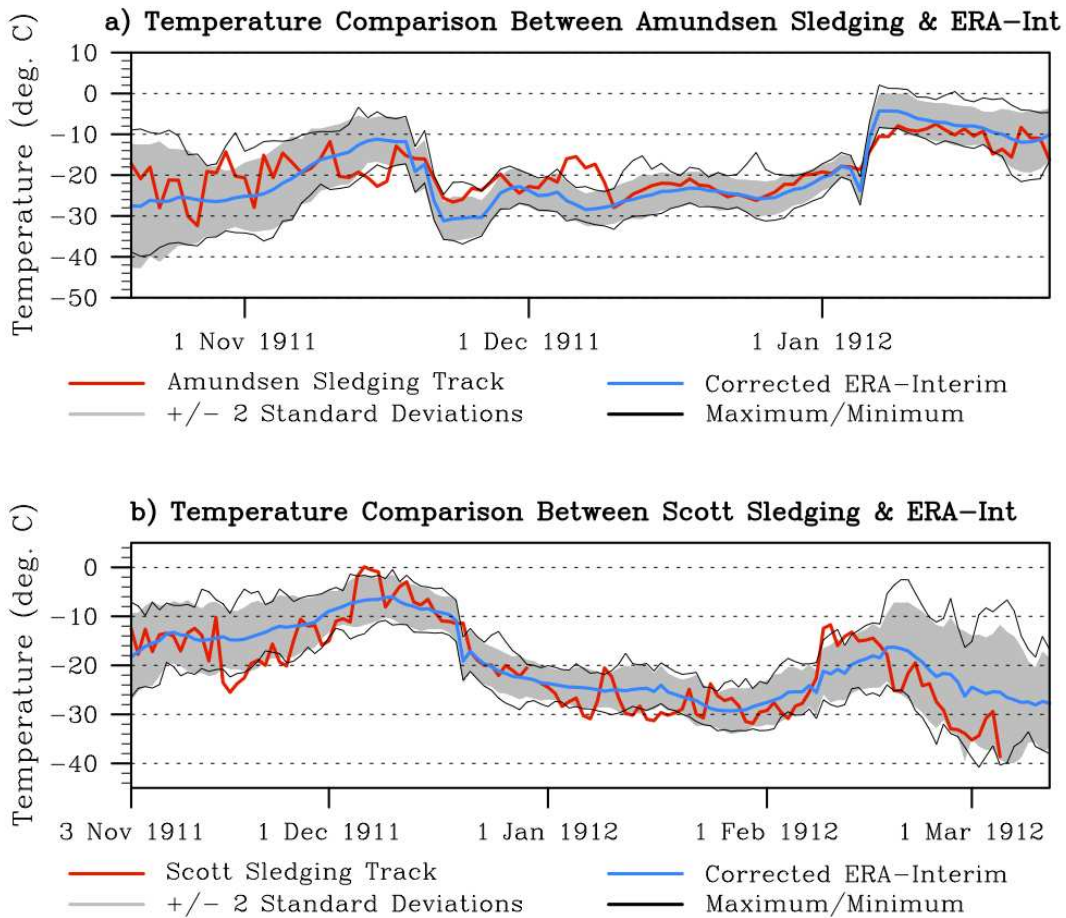


Elevation (m)

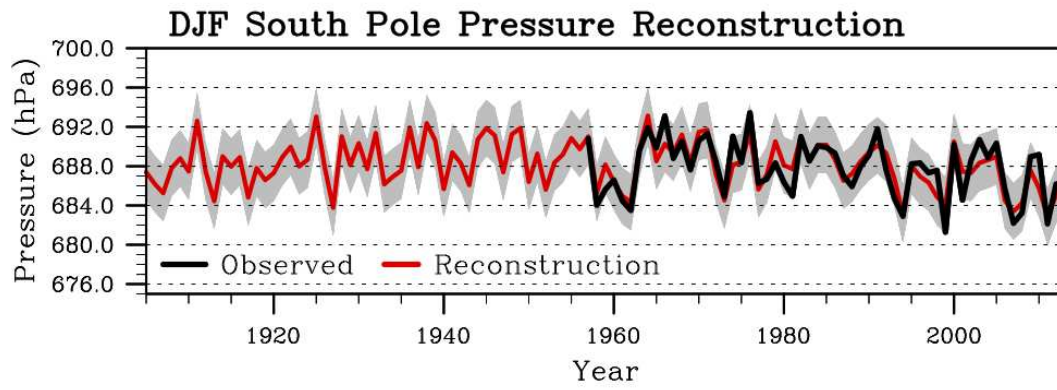


0 400 800 1200 1600 2000 2400 2800 3200 3600 4000

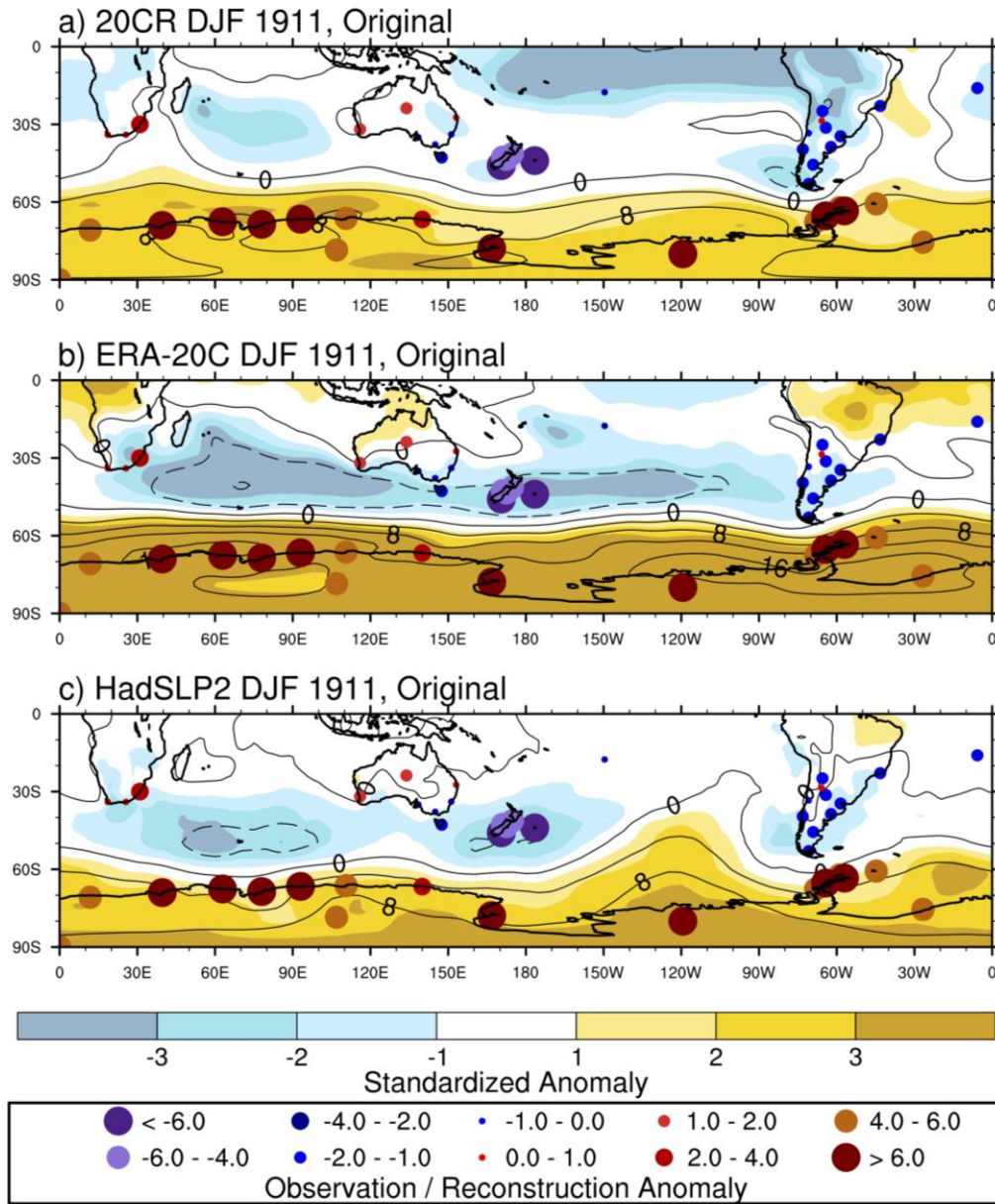
129 **Figure S3.** Model elevation for ERA-Int at the $0.75^\circ \times 0.75^\circ$ longitude-latitude resolution,
130 based on the invariant variable geopotential. Along the Transantarctic mountains,
131 elevations are greatly smoothed compared to the real world (Fig. 1 from main paper) and
132 no glacier valleys exist. Therefore elevation corrections to temperature are required.



133 **Figure S4.** Comparison of temperature observations along the sledging journey for a)
 134 Amundsen and b) Scott along with the elevation-adjusted ERA-Int climatological daily
 135 mean temperature (blue line). The daily mean temperature variability is represented by
 136 the ± 2 standard deviation ERA-Int daily mean temperature envelope (gray shading) and
 137 the maximum / minimum ERA-Int daily mean temperature (think black lines).
 138

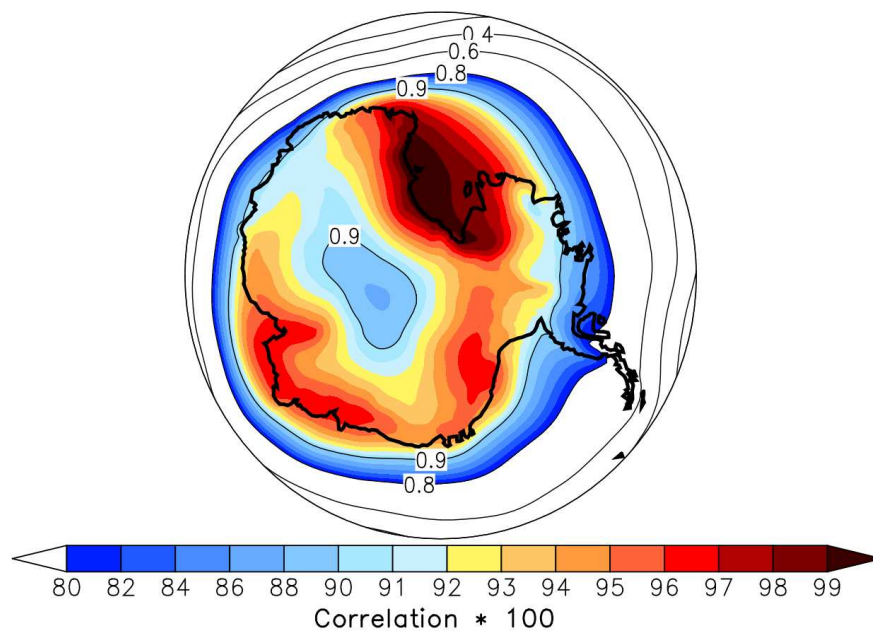


139 **Figure S5.** Summer (December-February) Amundsen-Scott South Pole station observed
140 (black) and reconstructed (red) surface pressure. Also plotted is the 95% confidence
141 interval for the reconstruction, which correlates with the observations at $r=0.859$.
142

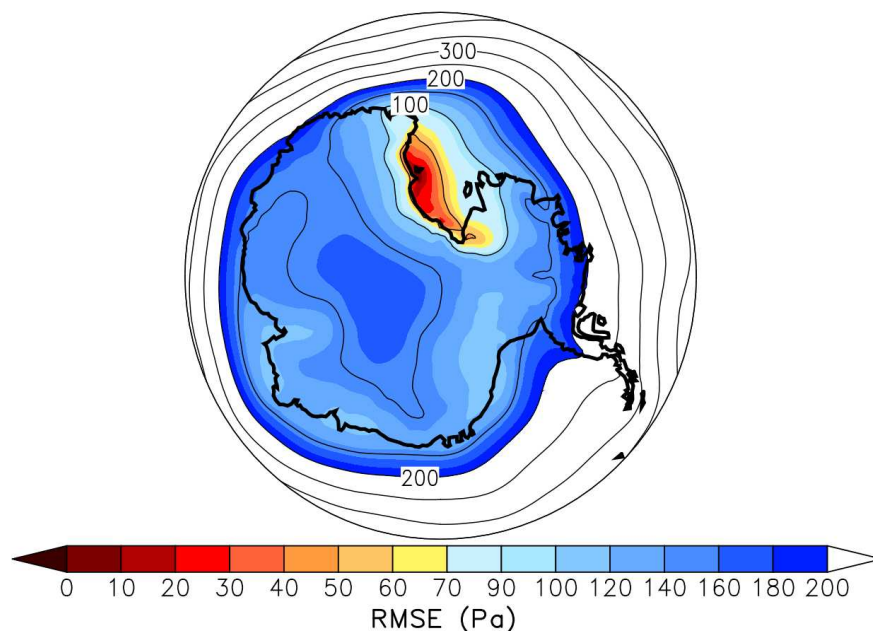


143 **Figure S6.** DJF 1911/12 pressure anomalies and standard deviations (contoured and
 144 shaded, respectively) from the 1981-2010 climatological mean for a) 20CR b) ERA-20C
 145 and c) HadSLP2, along with circles indicating observed midlatitude pressure anomalies
 146 (equatorward of 60°S) and Antarctic pressure reconstruction anomalies (poleward of
 147 60°S), with anomaly magnitude given by the legend.
 148

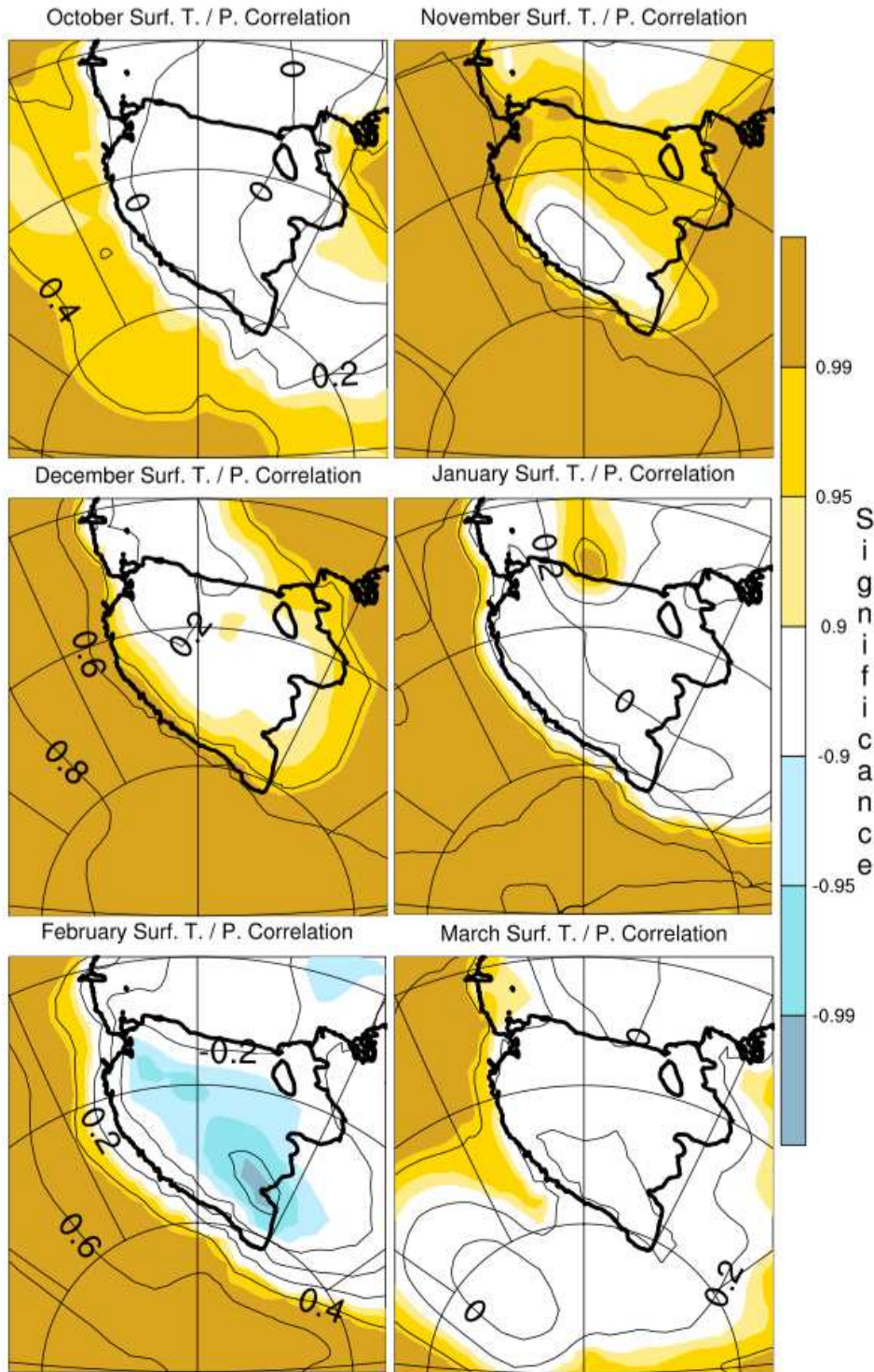
McMurdo Correlation



McMurdo RMSE

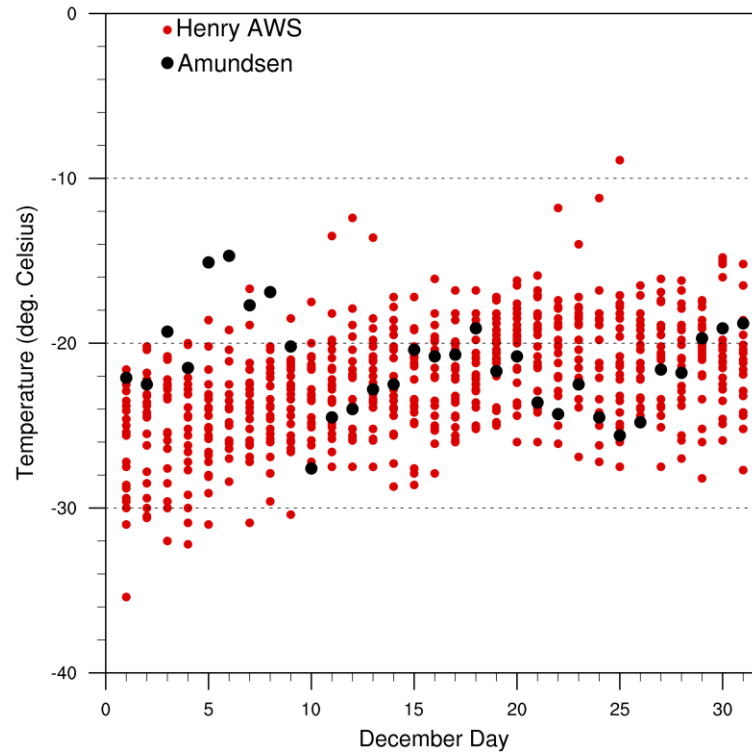


149 **Figure S7.** Top: Correlation of the pressure at McMurdo station with every other grid
150 point of the ERA-Int surface pressure anomalies during DJF. Pressure correlations on the
151 Ross Ice Shelf exceed 0.95 everywhere, and are above 0.99 for much of the western Ross
152 Ice Shelf along Scott's route. Bottom: The root mean squared error (RMSE, in Pa)
153 between McMurdo pressures and every other grid point of the ERA-Int surface pressure
154 anomalies during DJF. Again, across the Ross Ice Shelf the mean error is less than 1 hPa,
155 and less than 0.5 hPa in the western Ross Ice Shelf along Scott's route.

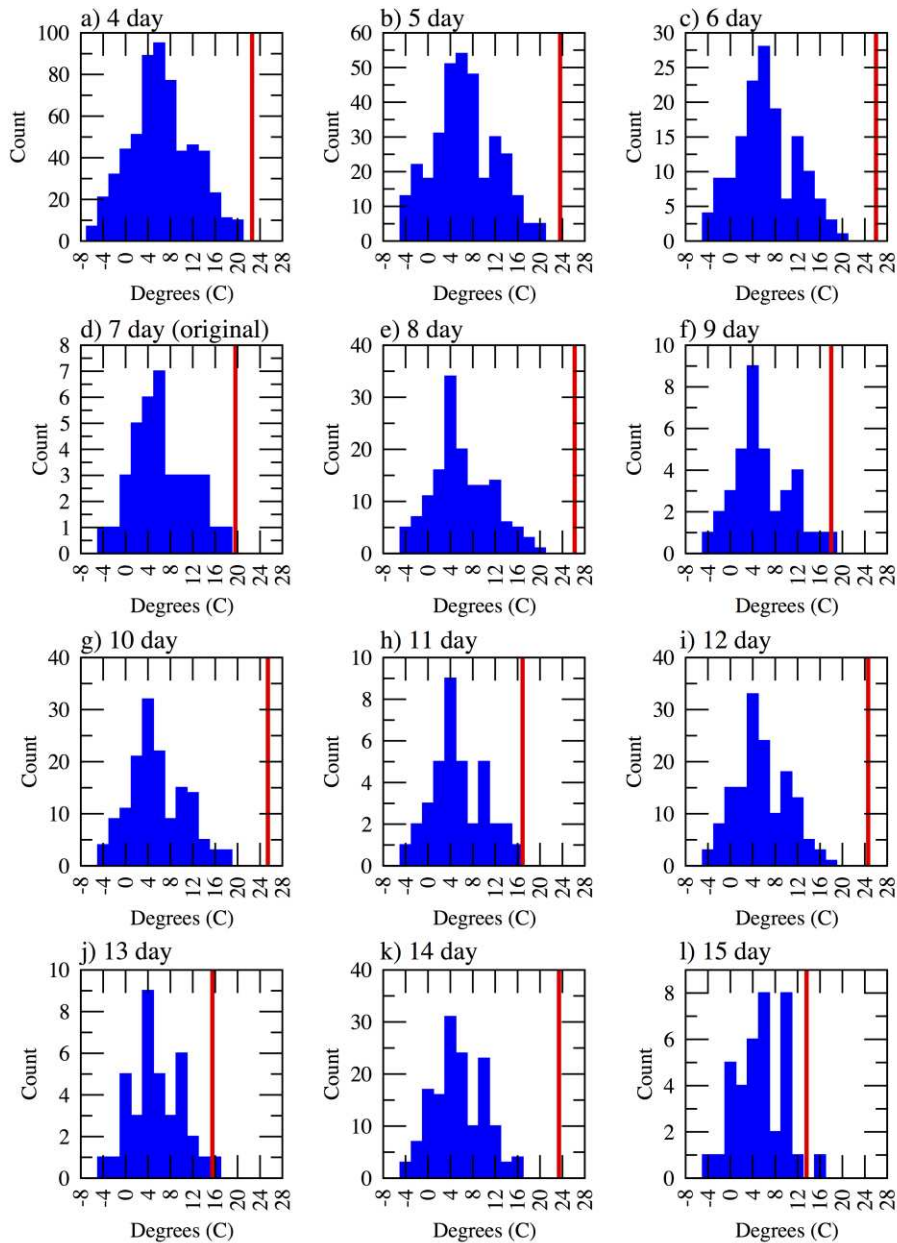


156 **Figure S8.** Monthly (October- March) surface pressure and temperature correlation maps
 157 during 1979-2015 at every gridpoint from ERA-Interim $0.75^{\circ} \times 0.75^{\circ}$ data. Shading
 158 represents the statistical significance of the monthly correlations, as given by the label bar
 159 on the right $(1-p) \times 100$, and negative for negative correlations; white areas indicate
 160 regions of $p > 0.10$.

Henry AWS (1993-2015) vs. Amundsen (1911) Max Daily Temperature



161
162 **Figure S9.** Daily maximum temperatures from the Henry automatic weather station (red)
163 during 1993-2015, based on quality controlled 10-minute data, and the 1911 Amundsen
164 daily maximum temperatures (black).
165



166
 167 **Figure S10.** Histograms of absolute temperature difference from February 9-15 and
 168 February 27 – March 5, based on varying lengths of number of days for averaging in both
 169 the earlier and later periods (indicated by individual panel titles), from ERA-Interim daily
 170 temperature data during 1979-2015. The red vertical line indicates the mean temperature
 171 difference experienced by Scott in 1912.